Bowing effect in elastic constants of dilute Ga(As,N) alloys

Jonas Berggren, Michael Hanke, and Achim Trampert

Citation: Applied Physics Letters **108**, 183106 (2016); doi: 10.1063/1.4948935
View online: http://dx.doi.org/10.1063/1.4948935
View Table of Contents: http://scitation.aip.org/content/aip/journal/apl/108/18?ver=pdfcov
Published by the AIP Publishing

Bowing effect in elastic constants of dilute Ga(As,N) alloys

Jonas Berggren, Michael Hanke, and Achim Trampert[a)]
Paul-Drude Institut für Festkörperelektronik, Hausvogteiplatz 5–7, D-10117 Berlin, Germany

(Received 10 February 2016; accepted 27 April 2016; published online 5 May 2016)

We study the elastic properties of dilute Ga(As,N) thin films grown on GaAs(001) by means of nano-indentation and complementary dynamic finite element calculations. The experimental results of indentation modulus are compared with simulations in order to extract the cubic elastic constants c_{ij} as a function of nitrogen content of the Ga(As,N) alloys. Both, indentation modulus and elastic constants decrease with increasing nitrogen content, which proves a strong negative bowing effect in this system in contrast to Vegard's law. *Published by AIP Publishing.*
[http://dx.doi.org/10.1063/1.4948935]

Ternary Ga(As,N) alloys are characterized by a large miscibility gap, limiting the range of forming homogeneous ternary compounds to a few per cent only. These alloys are especially suitable for optoelectronic devices approaching the technologically highly relevant telecom wavelengths 1.3 and 1.55 μm.[1] Besides that, Ga(As,N) has been considered as a material for spintronics[2] and solar cell applications.[3]

A large decrease in band gap of almost 30% compared to GaAs has been reported for the incorporation of only 4% of nitrogen into Ga(As,N), which corresponds to a large deviation from the linear relationship between composition and band gap variation.[4] The proposed reason is that the replacement of the As atom with the much smaller and more electronegative N atom leads to a large perturbation of the crystal lattice potential, resulting in an anti-crossing interaction between the localized N states and the extended conduction-band states. Consequently, the result is a splitting of the conduction band which leads to a decrease of the band gap.[5] These general properties of dilute nitrides are well investigated; however, less is known about the elastic behavior of Ga(As,N) alloys. First principle calculations of the mechanical and structural properties of Ga(As,N)[6] reveal a negative bowing for the cubic elastic constants c_{11}, c_{12}, and c_{44} as a function of the nitrogen content in contrast to Vegard's law, i.e., to the linear correlation between both limiting binaries GaAs and GaN (metastable cubic crystal structure). On the contrary, such deviations are not observed in measurements of the ternary semiconductor alloys $Al_{1-x}Ga_xN$[7] and $In_xGa_{1-x}As$,[8] where size differences of the atoms are smaller and the formation of interstitials is hardly possible.

In this letter, we report on a non-linear dependence of elastic constants in Ga(As,N) alloys as a function of nitrogen content. Therefore, we have determined elastic properties by a combination of nano-indentation experiments with numerical finite element method (FEM). The experimentally derived indentation moduli of epitaxially grown $GaAs_{1-x}N_x$/GaAs(001) heterostructures with different dilute compositions of $x < 0.025$ are compared with simulated indents. In an iterative approach, FEM simulations are improved and thus yield (by comparison with the experiment) the elastic properties, i.e., the cubic elastic constants c_{11}, c_{12}, c_{44} of Ga(As,N) as a function of nitrogen content.

The Ga(As,N) films were grown by molecular beam epitaxy (MBE) on GaAs(001) substrates using an RF plasma source for N supply. A conventional Knudsen Ga effusion cell was used, where the beam equivalent pressure (BEP) is controlled by regulating the cell temperature. The As was supplied by a valved cracker cell which allows for a direct and precise control of the As flux. The most important growth parameters are the substrate temperature, the plasma power, and the V/III BEP-ratio. All these parameters govern the incorporation of nitrogen during MBE. Previous studies indicate that homogeneous Ga(As,N) layers can be grown under conditions of either low V/III BEP-ratio of 3–4 and low growth temperatures or high V/III BEP-ratio of 25–50 in combination with high temperatures.[9]

In the following, the option with high BEP-ratio was selected for the growth and the substrate temperature was set to 460 °C for all samples. Reflection high-energy electron diffraction (RHEED) was used to monitor the MBE growth *in-situ*, confirming a smooth two-dimensional growth front resulting in an atomically smooth surface. Two sets of samples were grown with nominal nitrogen content of 1.4% and 2.3% where the layer thickness is varied between 50 nm and about 500 nm within each series. The compositions of the alloys were determined by X-ray diffraction[10] around the symmetric (004) and asymmetric (224) reflections in order to take into account the changes of the lattice parameters due to both composition and strain. The variation in composition over each set of samples amounts to about $\pm 0.2\%$.

Indentation modulus measurements were performed using the nano-indentation system MTS XP equipped with a Berkovich type diamond indenter tip. During indentation, the tip penetrates into the material to a certain pre-defined depth (loading) and is subsequently withdrawn (unloading). A plastic zone of high dislocation density is created during loading, whereas the restoring forces around the plastic zone react upon the tip withdrawal. This elastic reaction corresponds to the indentation stiffness of the material, which is defined as the slope of the load-displacement curve at the beginning of unloading, $S = dP/dh$, where P is the load of the indenter on the sample and h the corresponding indentation depth. From this measured value of S, a reduced indentation

[a)]trampert@pdi-berlin.de

modulus M^* of the tip and the sample can be determined according to[11]

$$M^* = \frac{1}{2}\frac{\sqrt{\pi}}{\sqrt{A(h)}}\frac{1}{\beta}S, \tag{1}$$

with $A(h)$ as the projected area of the indentation at the contact depth h. It is approximated from an established calibration procedure that determines the relation between the projected area A and the indentation depth h.[12] The fixed maximal indentation depth of $h_{max} = 70$ nm is used for all indents related to this work. The parameter β is a constant which depends on the geometry of the indenter tip ($\beta = 1.096$ for a Berkovich tip[11]). To take into account the influence of the tip, the indentation modulus M_c of the Ga(As,N)/GaAs composite material is derived from the reduced modulus M^* by

$$\frac{1}{M^*} = \frac{1-\nu_t^2}{M_t} + \frac{1-\nu_c^2}{M_c}. \tag{2}$$

The subscripts t and c denote the indenter tip and the sample (composite) material, respectively, and $\nu_{t,c}$ are the corresponding Poisson's ratios. The parameters of the diamond indenter used were $M_t = 1147$ GPa and $\nu_t = 0.07$. Here we assume for the composite material $\nu_c = \nu_{GaAs} = 0.31$, while for all FEM calculations the full elastic anisotropy of both materials (layer and substrate) and hence different Poisson ratios are considered.

All indentation measurements presented in this paper were carried out by the so-called continuous stiffness method (CSM) to measure the indentation modulus M_c *continuously* as a function of the indentation depth h. This method proposed by Oliver and Pharr[12] is favorably applied for analysis of thin films since it performs with very small oscillations of the indenter tip during penetration with a frequency of 50 Hz and an amplitude of 2 nm. To improve statistics, all indentation measurements were repeated ten times at each sample and the given moduli are the resulting average.

Figure 1 shows the indentation modulus M_c as a function of indentation depth h measured by CSM for two Ga(As,N)/GaAs heterostructures with N content of 1.4% and 2.3%, respectively, and for the bare GaAs substrates as reference. All indents are made to a maximum depth of only 70 nm, i.e., this depth is much smaller than the film thickness of 400 nm, $h \ll t$. For very shallow indents, less than 10 nm, the indentation modulus is determined by surface-related phenomena such as the pile-up effect or imperfections in the shape of the indenter tip.[11]

The subsequent, almost flat regime of each curve between 40 nm and 65 nm is taken to define the indentation modulus M_c of the entire heterostructure. In case of pure GaAs, the indentation modulus is determined to be 126.2 GPa, in good agreement with the literature values.[8] Furthermore, the measurements in Fig. 1 clearly demonstrate the remarkable trend that the indentation modulus M_c of Ga(As,N)/GaAs heterostructures decreases with increasing N content, starting from 124.4 GPa for [N] = 1.4 ± 0.2% towards 121.2 GPa in case of [N] = 2.3 ± 0.2%. Based on a linear behavior, one might expect the opposite, since the modulus of cubic GaN ($M \approx 262$ GPa)[13] is considerably larger than that of GaAs. In order to discuss this rather unexpected elastic property of the layer independent of the substrate, one has to disentangle both contributions to the composite value M_c.

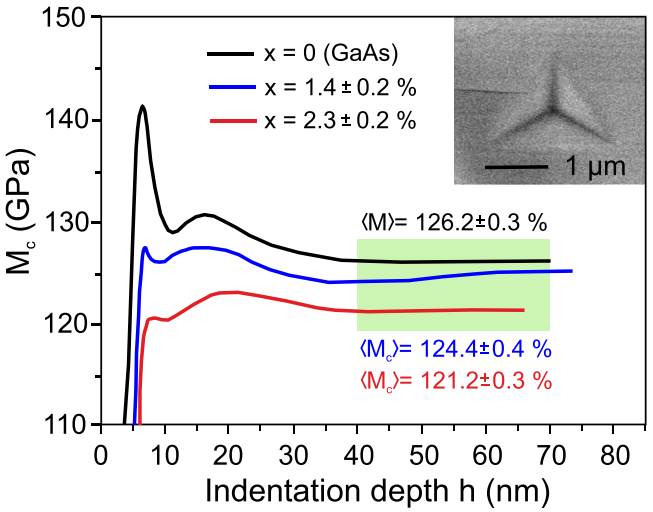

FIG. 1. Indentation modulus M_c for two Ga(As,N)/GaAs heterostructures (composite values) and for bare GaAs substrate. The flat regions beyond $h = 40$ nm provide reliable results independent of pile-up effects visible at small indentation depths at the beginning of all curves. The inset shows a scanning electron micrograph of the sample surface after indentation.

Although the indentation depths in Fig. 1 are small compared to the film thickness, a residual influence of the substrate remains certainly present. In order to consider this tiny effect, and eventually to correct the composite value M_c, we have performed systematic indents of maximal depth $h_{max} = 70$ nm on a series of heterostructures with increasing film thickness t while keeping the chemical composition constant. The measured data points plotted in Fig. 2(a) show the experimental indentation moduli for two sets of Ga(As,N)/GaAs heterostructures with nitrogen contents of 2.3 ± 0.2% and 1.4 ± 0.2% and layer thicknesses between 150 and 500 nm. Noteworthy to say, each data point represents an averaged value of 20 CSM measurements with error bars displaying the standard deviation. The values at $t = 0$ (pure GaAs) and $t = 400$ nm, respectively, correspond to the data presented in Fig. 1. The measured composite moduli M_c decrease with film thickness, Fig. 2(a), indicating different moduli for film, M_f, and substrate, M_s.

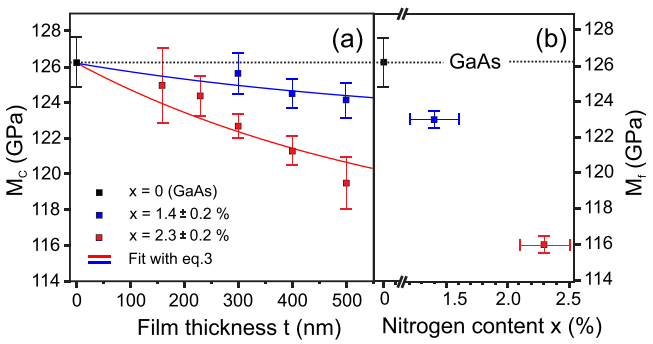

FIG. 2. (a) Composite indentation moduli M_c versus film thickness t for two sets of samples with different nitrogen content. (b) Intrinsic film indentation moduli M_f.

In the limit of a vanishing (infinite) layer thickness $t = 0$ ($t \to \infty$), M_c will approach M_s (M_f), respectively. There are several methods in the literature to determine the *intrinsic* film modulus E_i. Here, we follow the method introduced by Doerner and Nix,[14] where the elastic behavior of film and substrate is described by two springs with different spring constants so that the following relation is empirically derived as:

$$\frac{1}{M_c} = \frac{1}{M_f} + \left(\frac{1}{M_s} - \frac{1}{M_f}\right) e^{-\alpha(t/h)}, \tag{3}$$

where α describes an empirical constant.

The data points of the two sets of samples [red and blue squares in Fig. 2(a)] can be fitted by Eq. (3) taking into account the modulus of pure GaAs ($M_s = 126.2$ GPa), yielding the constant $\alpha = 0.10$ and the inherent film modulus M_f. The resulting values for the M_f are 123 ± 0.5 GPa and 116 ± 0.5 GPa for [N] $= 1.4 \pm 0.2\%$ and $2.3 \pm 0.2\%$, respectively, which means that a larger nitrogen content implies a smaller elastic film modulus in accordance to the trend of the indentation modulus of the heterostructures. It should be noted, however, that the film modulus M_f is not exactly equal to a hypothetical bulk modulus of the corresponding Ga(As,N) alloy, since there is also epitaxial strain involved in the case of a film on a substrate, which might additionally affect the modulus measurement.

There is a large decrease of about 8% for the incorporation of 2.3% nitrogen compared to pure GaAs, Fig. 2(b). This reduction is a strong discrepancy from the alloying behavior based on Vegard's law, which considers a linear interpolation between the two binaries GaAs ($M = 126.2$ GPa) and cubic GaN ($M \approx 262$ GPa),[13] and thus predicts an increase with increasing N content. The decrease in M_f and the deviation from Vegard's law can be explained as originating from a weakening of Ga-N bonds due to the large strain emerging from the size differences between the As and N atoms in the case of a regular substitution, where an As atom is replaced by an N atom in the crystal lattice. Furthermore, the small size of the N atom enables the formation of N-N and N-As *molecular* interstitials,[6] which can occupy sites generally reserved by single As atoms. These configurations weaken the Ga-N bond strength, because the N in this case is three-fold coordinated to Ga compared to the normal four-fold bonding.

All FEM simulations have been performed with the commercial software package MarcMentat®. Here, the process of indentation can be treated in a so-called contact problem made of two entities: the movable indenter and the rigid heterostructure itself. Although a numerical approach as FEM enables various geometries for both, we restrict ourselves to an axis-symmetric problem, which in particular, includes a spherical indenter shape [cf. Fig. 3(a)]. Based on that there are two classes of input parameters, first the morphology of the film-substrate heterostructure. This covers the respective cubic elastic constants c_{11}, c_{12}, and c_{44}, the yield stress, τ_{Yield}, for the inset of plastic relaxation of the Ga(As,N) film, and finally the GaAs(001) substrate. Second, we have chosen a spherical diamond tip with a radius of 300 nm, which is incrementally penetrating the heterostructure. This particular radius corresponds approximately to the similar contact area that can be attributed to a Berkovich tip when penetrating 70 nm into the surface.

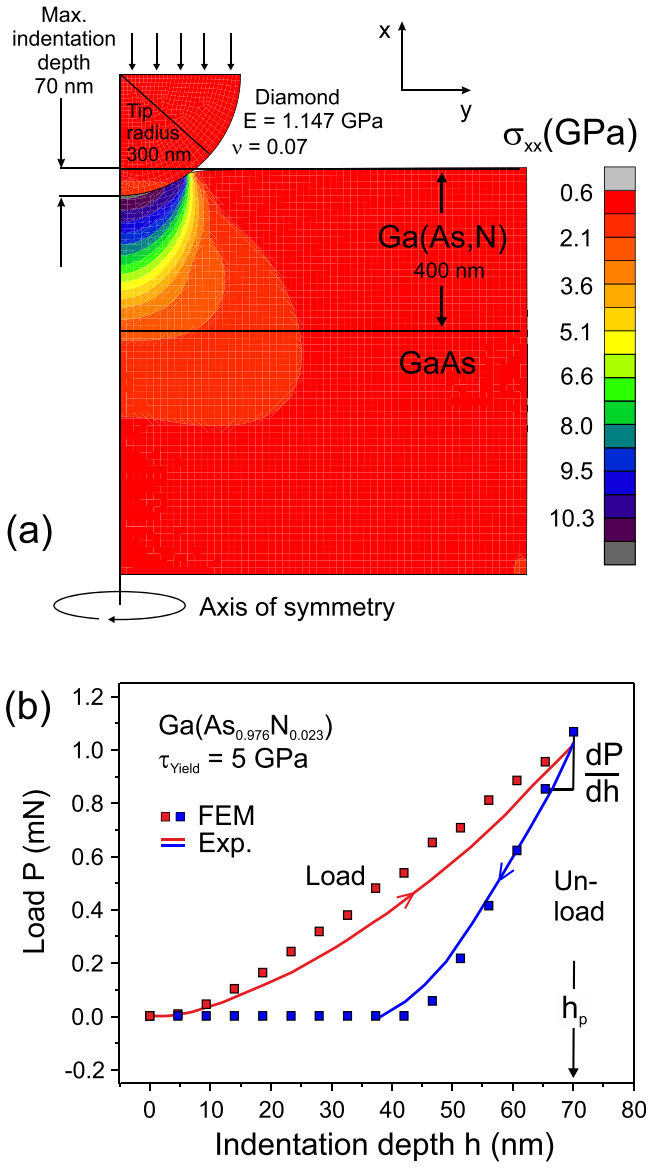

FIG. 3. (a) Axis-symmetric finite element calculation at the turning point from load to unload showing the vertical component σ_{xx}. Here, we considered a 400 nm thick Ga(As,N) layer on top of a GaAs(001) substrate indented by a spherical diamond tip with 300 nm radius up to a maximum depth of 70 nm. The dots in (b) give the applied load P at each increment during load and unload, while the blue and red lines show a comparable experimental load-unload experiment.

Figure 3(b) represents the *dynamics* during load and unload at the example of a load-displacement (P–h) curve up to a maximum penetration depth of 70 nm. In fact, the *static* two-dimensional profile of the stress component σ_{xx} at the turning point from load to unload is shown in Fig. 3(a). The indentation load P for a given depth h is numerically obtained by integrating the normal stress component σ_{xx} over the whole contact area between tip and sample surface. The quality of the FEM indentation simulation is tested with GaAs(001) assuming the following elastic constants: $c_{11} = 119.0$ GPa, $c_{12} = 54.0$ GPa, and $c_{44} = 59.5$ GPa.[15] The maximum depth of 70 nm is achieved by a load of 1.08 mN and a yield stress of 5 GPa is selected to gain the residual impression of 40 nm, as seen in Fig. 3(b).

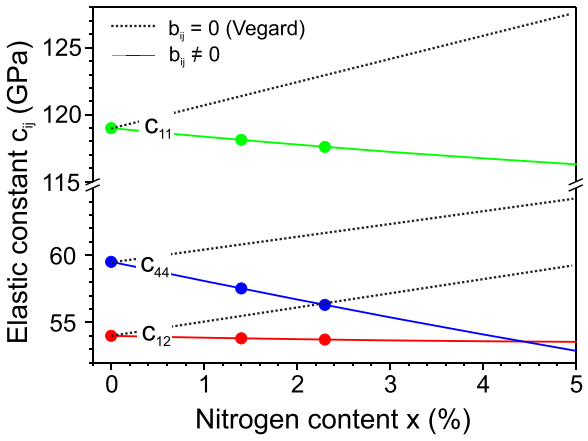

FIG. 4. Elastic constants c_{ij} of Ga(As,N) extracted from FEM simulations show a large negative bowing compared to what would be expected by linear alloying behavior based on Vegard's law.

Finally, the elastic constants of the sample are varied until the load-displacement curve and thus the calculated stiffness $S^{sim} = dP/dh$ and indentation modulus M_f^{sim} match the experimental result according to Eq. (1). The simulation is made with a spherical tip instead of the experimentally used three-sided Berkovich pyramid, and furthermore, the stiffness $S = dP/dh$ is calculated from the unloading of the tip as displayed in Fig. 3, and not from a CSM measurement as in the experiment. Under these conditions, we could use a parameter $\beta = 1.000$ in the FEM calculation, which reasonably considers the indenter tip geometry.

The elastic constants of cubic Ga(As,N) alloys, c_{ij}, are defined as

$$c_{ij}^{Ga(As,N)} = (1-x)\cdot c_{ij}^{GaAs} + x\cdot c_{ij}^{GaN} - b_{ij}\cdot x(1-x), \quad (4)$$

where x is the nitrogen concentration [i.e., $0 \le x \le 1$], and b_{ij} are the so-called bowing coefficients describing the deviation from the linear interpolation between the elastic constants of the binaries GaAs and GaN. In order to reduce the number of independent elastic constants (c_{11}, c_{12}, and c_{44}) in the FEM simulation, we introduce the following assumptions for the ratios b_{ij} [see Refs. 6 and 16], respectively: $b_{11}/b_{12} \approx 2$, $b_{11}/b_{44} \approx 1$. Accordingly, by fixing the parameter c_{11} in the simulation, the two coefficients c_{12} and c_{44} are calculated using Eq. (4).

Figure 4 summarizes the results for c_{11}, c_{12}, and c_{44} of Ga(As,N) films as a function of the nitrogen concentration. Assuming an alloying behavior based on Vegard's law [i.e., $b_{ij} = 0$], a linear increase of c_{ij} is calculated by Eq. (4), connecting the values for the binary GaAs and GaN. Taken our FEM simulations of the experimental indentation moduli, we obtain a strong negative bowing [$b_{11} = b_{44} = 240$ GPa, $b_{12} = 120$ GPa] in the dilute regime, which is more pronounced than predicted by density functional theory (DFT) calculations [$b_{11} = 156$ GPa, $b_{12} = 88$ GPa, and $b_{44} = 166$ GPa].[6]

We would like to mention that a quantitative comparison between the results and the DFT is problematic since we limited ourselves to fixed ratios for the bowing coefficients. Most likely, the strong negative bowing is related to the incorporation of N_2 interstitials in GaAs, which are energetically favorable[6] due to the comparatively small size of a nitrogen atom.

In conclusion, we present experimental results on indentation moduli M of Ga(As,N) layers based on nano-indentation. A decrease of M with increasing nitrogen content compared to pure GaAs has been observed. Complementary dynamic FEM simulations of the nano-indentation process yield the elastic constants c_{11}, c_{12}, c_{44} as a function of nitrogen content in Ga(As,N), a relation which has been described by a quadratic term additional to the linear dependence of Vegard's law. These investigations prove a pronounced negative bowing for elastic constants vs. nitrogen content in the case of Ga(As,N). We refer this observation to the incorporation of N atoms in GaAs as interstitial substitution.

We would like to thank Bernd Jenichen for giving a comprehensive introduction into the used x-ray equipment.

[1]J. S. Harris, Jr., Semicond. Sci. Technol. **17**, 880 (2002).
[2]H. M. Zhao, L. Lombez, B. L. Liu, B. Q. Sun, Q. K. Xue, D. M. Chen, and X. Marie, Appl. Phys. Lett. **95**, 041911 (2009).
[3]B. Bouzazi, K. Nishimura, H. Suzuki, N. Kojima, Y. Ohshita, and M. Yamaguchi, Curr. Appl. Phys. **10**, S188 (2010).
[4]K. Uesugi, I. Suemune, T. Hasegawa, T. Akutagawa, and T. Nakamura, Appl. Phys. Lett. **76**, 1285 (2000).
[5]W. Shan, K. M. Yu, W. Walukiewicz, J. Wu, J. W. Ager III, and E. E. Haller, J. Phys.: Condens. Matter **16**, S3355 (2004).
[6]G. Stenuit and S. Fahy, Phys. Rev. B **76**, 035201 (2007).
[7]D. Cáceres, I. Vergara, R. Gonzáles, E. Monroy, F. Calle, E. Muñoz, and F. Omnès, J. Appl. Phys. **86**, 6773 (1999).
[8]S. Korte, I. Farrer, and W. J. Clegg, J. Phys. D: Appl. Phys. **41**, 205406 (2008).
[9]F. Ishikawa, E. Luna, A. Trampert, and K. H. Ploog, Appl. Phys. Lett. **89**, 181910 (2006).
[10]M. E. Vickers, M. J. Kappers, T. M. Smeeton, E. J. Thrush, J. S. Barnard, and C. J. Humphreys, J. Appl. Phys. **94**, 1565 (2003).
[11]A. C. Fischer-Cripps, Surf. Coat. Technol. **200**, 4153 (2006).
[12]W. C. Oliver and G. M. Pharr, J. Mater. Res. **7**, 1564 (1992).
[13]J. Pezoldt, R. Grieseler, T. Schupp, D. J. As, and P. Schaaf, Mater. Sci. Forum **717**, 513 (2012).
[14]M. F. Doerner and W. D. Nix, J. Mater. Res. **1**, 601 (1986).
[15]S. Adachi, J. Appl. Phys. **58**, R1 (1985).
[16]M. Reason, X. Weng, W. Ye, D. Dettling, S. Hanson, G. Obeidi, and R. S. Goldman, J. Appl. Phys. **97**, 103523 (2005).